engineering proceedings

MDPI

Proceeding Paper

Modeling and Numerical Simulation of a $CH_3NH_3SnI_3$ Perovskite Solar Cell Using the SCAPS1-D Simulator †

Selma Rabhi [1,2,*], Hichem Benzouid [3], Abdelhadi Slami [4] and Karima Dadda [1]

[1] Semiconductor Materials Laboratory and Metal Oxides, University of Science and Technologie Haouri Boumedien, B.P. 32, El Alia, Bab Ezzouar, Algiers 16111, Algeria; daddakarima21@gmail.com
[2] Mechanical Engineering Department, Faculty of Technology, YAHIA Fares University, Medea 26000, Algeria
[3] Laboratory of Metallurgy and Materials Engineering, University of Badji Mokhtar(UBMA), Annaba 23000, Algeria; hichembenz25@gmail.com
[4] Material and Renewable Energy Research Unit (URMER), University of Tlemcen, Tlemcen 13000, Algeria; slamiabdelhadi@gmail.com
* Correspondence: selma.rabhi@ensmm-annaba.dz or rabhi.selma@univ-medea.dz
† Presented at the 4th International Electronic Conference on Applied Sciences, 27 October–10 November 2023; Available online: https://asec2023.sciforum.net/.

Abstract: In this work, our aim was to design and numerical simulation of a solar cell using the SCAPS-1D simulation program. The studied solar cell has an N-I-P type structure, with its active layer based on a hybrid (organic–inorganic) semiconductor called "methylammonium tin triiodide perovskite", $CH_3NH_3SnI_3$, which is known as $MASnI_3$. This semiconductor is known for its efficiency in the field of photovoltaic thanks to its good properties such as high absorption, direct bang-gap, and facilities of elaboration. The objective of this study was primarily focused on improving the performance of the perovskite solar cells, specifically enhancing their reproducibility and stability, as they tend to degrade rapidly. To achieve this, we proposed the use of ZnO and Spiro-OMeTAD as charge transport layers (ETL and HTL, respectively) and varying the thickness of the active layer to obtain the optimal parameters that ensure the proper functioning of the cell.

Keywords: SCAPS-1D; hybrid; perovskite; photovoltaics; ETL; HTL

Citation: Rabhi, S.; Benzouid, H.; Slami, A.; Dadda, K. Modeling and Numerical Simulation of a $CH_3NH_3SnI_3$ Perovskite Solar Cell Using the SCAPS1-D Simulator. *Eng. Proc.* **2023**, *56*, 97. https://doi.org/10.3390/ASEC2023-15300

Academic Editor: Simeone Chianese

Published: 26 October 2023

1. Introduction

The direction of the solar cell industry is to make solar cells more efficient and punchier at low cost. Perovskite-based solar cells could revolutionize this industry thanks to their interesting physico-chemical properties. The perovskite is the active layer in the solar cell, therefore, the coupling between the development and the study of the different properties of this layer in order to find the optimal conditions for the development of the perovskite layer contributes to the manufacture of an efficient solar cell [1]. Perovskite has a structure designated by the formula of AMX_3, where A is the cation (Cs, Rh, MA: CH_3NH_3 or else the FA: for $CH(NH_2)_2$, M is a cationic metal (Pb^{2+}, Sn^{2+}, Ge^{2+}), and X is an oxide or a halide (I, Br, Cl. . .). Its structure is an ionic structure, where the MX6 forms an octahedron with M located in the center of the octahedron and X is linked to the vertices of the cube around M. It is a tetragonal structure which contains an octahedral structure [2,3]. For these solar cells, the most commonly used component as the active layer is $CH_3NH_3PbI_3$, referred to as $MAPbI_3$, or methyl ammonium lead iodide. However, perovskites based on $MAPbI_3$ are toxic due to the presence of Pb, which can destabilize the continued commercialization of these cells. One of the alternative solutions is a perovskite material containing tin (Sn) instead of lead (Pb), known as methyl ammonium tin iodide ($CH_3NH_3SnI_3$ or $MASnI_3$. Many researchers have started to develop cells based on $CH_3NH_3SnI_3$, and this is what we also attempted to do [4]. Tin occurs naturally and has almost the same electronic properties as lead (Pb). Moreover, Sn-based perovskite solar cells (PSCs) exhibit good absorption in the

visible light spectrum and high charge mobilities, resulting in high solar cell efficiency [5–7]. The transport layers and the architecture also play a significant role in the efficiency of solar cells. In this work, we presented and discussed the results of our simulation for $CH_3NH_3SnI_3$-based PSCs.

2. Device Simulation Parameters

Numerical modeling has been shown to be beneficial for the investigation of the physical properties and construction of various solar cells made from different materials. Meanwhile, Solar Cell Capacitance Simulator SCAPS-1D (ELIS, University of Ghent, Belgium [8]) has demonstrated its efficacy in modeling a range of research systems, and it has become a widely used simulation tool for solar cell researchers due to its specialized functionality for semiconductor devices. A structure of the $CH_3NH_3SnI_3$-based PSC employed in this study is shown in Figure 1a, where the photovoltaic cell configuration is as follows. The ZnO/$CH_3NH_3SnI_3$/Spiro-OMeTAD/Au layers are stacked in the N-I-P structure. These materials exhibit favorable electronic properties, and the ETL and ZnO possess optical and electronic properties appreciated in the field of electronics. For the HTL, the most commonly used material in perovskite photovoltaic is Spiro-OMeTAD, as it is straightforward to implement and efficient in cells. However, the full device structure was simulated in SCAPS 1D by solving Poisson, electron, and hole continuity equations with inputs based on literature values (Table 1). The SCAPS-1D software (version.3.3.10) uses all the inputs to explore fundamental properties such as the short-circuit current J_{SC}, the open-circuit voltage V_{OC}, the power conversion efficiency of the device PCE, the quantum efficiency QE, and the fill factor FF.

Table 1. Input parameters of all layers in PSCs [9–12].

Parameters	ZnO	$CH_3NH_3SnI_3$	Spiro-OMeTAD
Thickness (nm)	500	450	0.350
Bandgap (eV)	3.47	1.3	3.2
Electron affinity (eV)	4.3	4.2	2.1
Dielectric permittivity (relative)	9	10	3
CB effective density of states ($1/cm^3$)	2×10^{18}	1×10^{19}	2.5×10^{18}
VB effective density of states ($1/cm^3$)	1.8×10^{20}	1×10^{18}	1.8×10^{19}
Electron thermal velocity (cm/s)	1×10^{7}	1×10^{7}	1×10^{7}
Hole thermal velocity (cm/s)	1×10^{7}	1×10^{7}	1×10^{7}
Electron mobility (cm^2/Vs)	1×10^{2}	1.6	2×10^{-4}
Hole mobility (cm^2/Vs)	2.5×10^{1}	1.6	2×10^{-4}
Shallow uniform acceptor density, N_A ($1/cm^3$)	0	$3 \times 10^{+15}$	$1 \times 10^{+20}$
Shallow uniform donor density N_D ($1/cm^3$)	$1 \times 10^{+19}$	$3 \times 10^{+15}$	0
Defect type	—	Neutral	Neutral
Capture cross section electrons (cm^2)	—	1×10^{-16}	1×10^{-15}
Capture cross section holes (cm^2)	—	1×10^{-16}	1×10^{-15}
Energy level with respect to reference (eV)	—	0.7	0.10
N_t total ($1/cm^3$) uniform	—	$4.5 \times 10^{+16}$	$1 \times 10^{+14}$

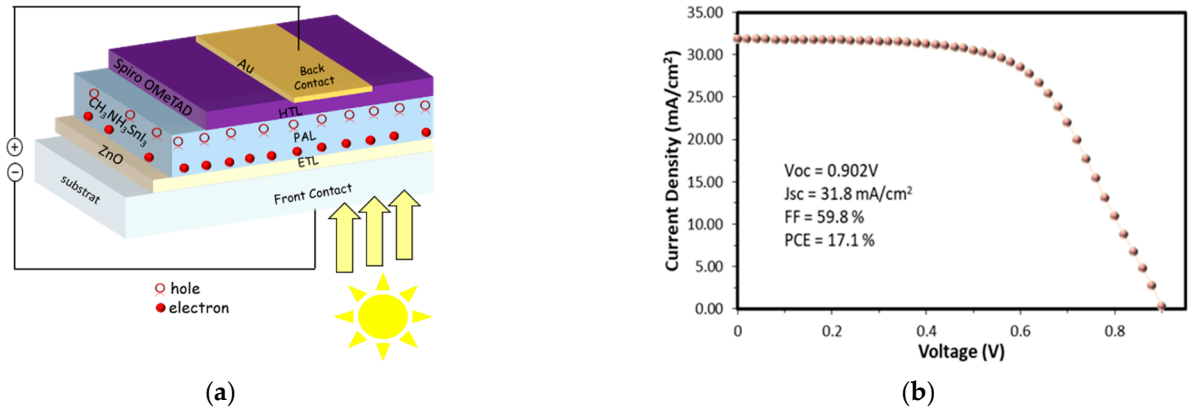

(**a**) (**b**)

Figure 1. (**a**) Schematic of the main device and (**b**) J-V characteristics of the $MAPbI_3$-based solar cell with the photovoltaic parameters.

Table 1 shows the input parameters of the layers that make up the perovskite solar cell; we used these inputs to extract the performance parameters of PSCs such as the J_{SC}, V_{OC}, FF, and PCE.

3. Results and Discussion

After selecting the input parameters of N-, I-, and P-layer that we need for SCAPS, we constructed the structure of the Sn-based PSC as presented in Figure 1a. The cell is illuminated from one side only (the front side on the HTL side), and we calculated the current–voltage density characteristic (J-V) for the very first time. Figure 1b, shows the current–voltage (J-V) characteristic of this cell under illumination by the AM 1.5 solar spectrum and a power density of 1000 w/m^2 [13]. From the J-V characteristics provided by SCAPS-1D in Figure 1b, we were able to determine photovoltaic performance such as J_{SC}, V_{OC}, FF, and PCE, where the PCE of this cell is = 17%, which means that the solar cell can convert only 17% of the light into usable electricity. This efficiency is low compared with the theoretical works on PSCs employing other materials such as ETL and the expectation for the $CH_3NH_3SnI_3$-based PSC. In recent times, Omarova et al. showed that the PSCs with $TiO_2/CH_3NH_3SnI_3/Cu_2O$ device structure offer an excellent PCE of ~27% [14]. Their results explain that the TiO_2-containing device efficiently decreases charge recombination, which means an enhancement in the PV performance. In addition, Hui-Jing Du et al., using TiO_2 as ETL with $CH_3NH_3SnI_3$ PSCs, offered a PCE of 23.36% after the optimization of PSC [15]. Otherwise, A V_{OC} of =0.9 V, represents the maximum voltage measured across the solar cell when no load is connected. An open circuit voltage is almost of the order and indicates that the solar cell is not capable of generating a significant voltage. However, A J_{SC} of almost 32 mA/cm^2 for a $CH_3NH_3SnI_3$-based PSC is generally considered to be quite good. However, FF of =60%: The fill factor is a measure of the solar cell's efficiency in terms of energy management. A FF of 60% is considered relatively low because it only exceeds the average by a small percentage and this shows that the solar cell is not using the available energy efficiently.

3.1. Performance of Optimized Parameters

Therefore, we will try to improve the performance of $CH_3NH_3SnI_3$-based PSC by optimizing some technological parameters of the absorber layer $CH_3NH_3SnI_3$ as it is the main layer in the whole cell. Therefore, we optimized the thickness of the $CH_3NH_3SnI_3$ active layer to have its best characteristics with the aim of enhancing the performance of the $CH_3NH_3SnI_3$-based PSC. We also simulated the effect of temperature on the complete solar cell. We varied the thickness of the $CH_3NH_3SnI_3$ active layer from 100 nm up to 900 nm in 100 nm increments.

To better visualize the effect of thickness on the performance of this photovoltaic cell, we plotted the four performances as a function of thickness. Figures 2–4 show these

performances (V_{OC}, J_{SC}, FF and PCE). Figure 2a shows the open circuit voltage as a function of the thickness of the $CH_3NH_3SnI_3$ active layer. We observe that this voltage increases as a function of thickness. This gradual increase in VOC with increasing layer thickness increases from 0.6774 V to 0.7568 V. This means that there is a positive correlation between the thickness of the active layer and the open circuit voltage. This correlation may be due to the charge transport properties or to better light capture by the active layer. This result is logical because of the good general electronic properties of the $CH_3NH_3SnI_3$ active layer. With regard to the second performance, Figure 2b also shows the evolution of the J_{SC} as a function of the thickness of the active layer. A steady increase in short circuit current is observed with increasing layer thickness, rising from 19.55 mA/cm^2 to 40.35 mA/cm^2 over a range from 50 nm to 900 nm. This could be explained by the fact that the cell with a thicker active layer contains a greater quantity of material capable of generating current in response to illumination.

The fill factor FF (%) is shown in Figure 3a, with an increase from 60.59% to 71.41%. This means that the cell with an active layer thickness of 900 nm converts light into energy at a rate of 71.41%. Now we come to the efficiency of the solar cell. As mentioned earlier, the PCE is a measure of the overall efficiency of a solar cell in converting light energy into electrical energy. The results presented in Figure 3b show a significant increase in efficiency with increasing film thickness, from 8.87% to 23.9%. This suggests that higher layer thicknesses can lead to better overall solar cell efficiency. Therefore, increasing the thickness of the $CH_3NH_3SnI_3$ active layer, which is the absorbing layer in the solar cell, results in better absorption of sunlight. This results in greater photon capture, which increases the number of electron–hole pairs generated. As a result, the amount of solar energy converted into electricity increases, which translates into an increase in the electrical current produced [16]. One of the positive results of increasing the thickness of the active layer is an increase in the diffusion time of charge carriers in the cell. This means that charge carriers have a greater chance of interacting with current collection sites, reducing recombination losses [17,18]. It is important to note that increasing thickness also has limits. Beyond a certain thickness, the effect of increasing thickness on efficiency can decrease, or even become negative, due to reduced charge carrier collection or other undesirable effects. Optimal photovoltaic cell design must consider these factors to maximize overall efficiency. The choice of ETL and HTL layers and even contact materials play a very important role in solar cell parameters; in this paper, we focused only on the effect of thickness on solar cell parameters [19]. As a result, these results indicate a correlation between the thickness of the $CH_3NH_3SnI_3$ active layer and the performance of the overall perovskite solar cell. A greater thickness favors higher values of open circuit voltage, short circuit current density, and overall efficiency. A good result is obtained for a $CH_3NH_3SnI_3$ active layer thickness of 900 nm, so this thickness is the optimum value where at this thickness the $CH_3NH_3SnI_3$-based PSC has good photovoltaic performance.

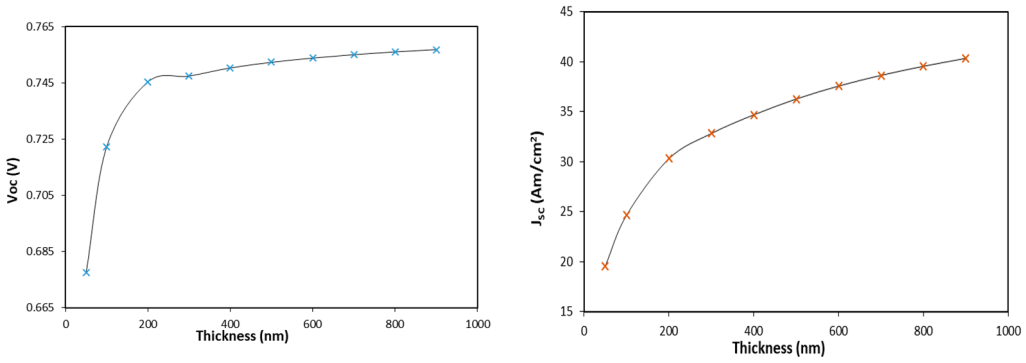

(**a**) (**b**)

Figure 2. (**a**) Presents the variation of open circuit voltage as a function of thickness and (**b**) presents a variation in current density as a function of thickness.

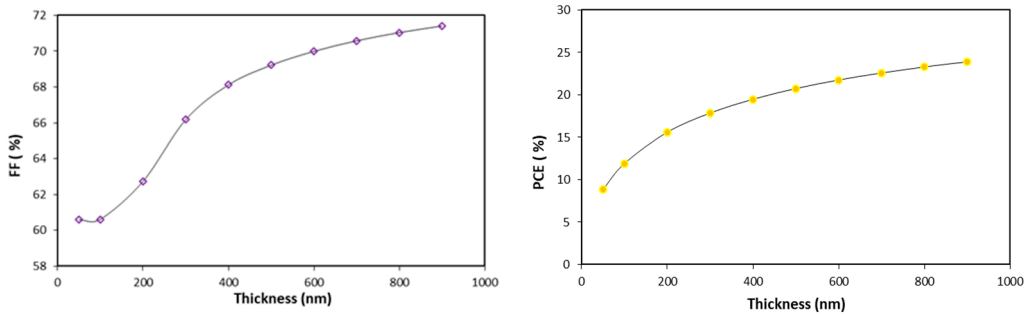

(**a**) (**b**)

Figure 3. The variation (**a**) of the fill factor as a function of thickness and (**b**) in power convention efficiency as a function of thickness.

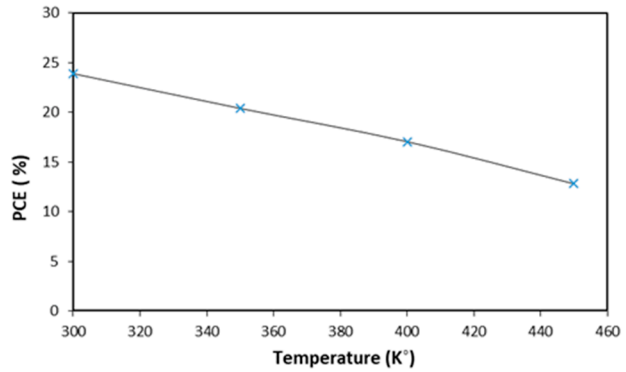

Figure 4. The influence of temperature increase on solar cell efficiency.

3.2. The Effect of Temperature on Solar Cell Efficiency

In this section, we analyze the effect of temperature on the efficiency of a perovskite solar cell with a $CH_3NH_3SnI_3$ active layer thickness of 900 nm. We varied the temperature from 300 K to 450 K with 50 K as steps. These results indicate that increasing temperature has a negative impact on the performance of the $CH_3NH_3SnI_3$-based PSC. Higher temperature leads to a decrease in V_{OC}, FF, and overall PCE. Although the short circuit current density appeared relatively stable, it can also show a slight decrease at higher temperatures. Figure 4 shows a significant decrease in PCE with increasing temperature. However, these results are consistent with the negative effects of temperature on the performance of perovskite-based solar cells; increasing temperature can have a significant negative impact on overall cell efficiency. One of the main reasons for this is that the $CH_3NH_3SnI_3$ layer is a temperature-sensitive material [18,20,21], which means that its optoelectronic properties are affected by temperature variations.

4. Conclusions

In this work, we modeled and optimized a $CH_3NH_3SnI_3$-based perovskite solar cell using ZnO and Spiro-OMeTAD as the electron and hole transport layers, respectively, using SCAPS software (version.3.3.10), and we identified an optimal thickness of 900 nm, which showed that the $CH_3NH_3SnI_3$ layer has excellent light absorption. The modeled cell achieved high power conversion efficiency exceeding 24%, an open-circuit voltage of 0.76 V, a short circuit current density of 40.35 mA/cm^2, and a fill factor of 71.41%. These high photovoltaic parameters demonstrate that CH3NH3SnI3-based PSCs can match or even surpass their $CH_3NH_3PbI_3$-based counterparts and satisfy environmental concerns by being environmentally friendly. The proposed model of a tin-based PSC had an absorbing layer thickness of 900 nm, which is more standard in terms of fabrication and intended for further application in the development of environmentally friendly and lead-free PSCs. With the further optimization of thermal stability, interface engineering, and geometry,

tin-based PSCs could become leading candidates for next-generation solar cells. The SCAPS simulations provide critical insights to guide the experimental development of efficient, stable, and eco-friendly tin-based PSCs.

Author Contributions: S.R.: Supervision, Validation, Visualization, Writing—original draft. H.B.: Data acquisition, Formal analysis, Writing—review & editing. A.S.: Data acquisition, Formal analysis, Validation, Visualization. K.D.: Resources, Visualization, Writing—original draft. All authors have read and agreed to the published version of the manuscript.

Funding: This research received no external funding.

Institutional Review Board Statement: Not applicable.

Informed Consent Statement: Not applicable.

Data Availability Statement: Data are available in this manuscript.

Acknowledgments: M Burgelman of the University of Gent in Belgium kindly provided the SCAPS-1 D program. The authors express their gratitude to him.

Conflicts of Interest: The authors declare no conflict of interest.

References

1. Rabhi, S. Etat de l' Art Des Couches Minces à Base Pérovskite Pour Des Applications Photovoltaïques Présenté Par. Master's Thesis, University of Constantine, Constantine, Algeria, 2015.
2. Kojima, A.; Teshima, K.; Shirai, Y.; Miyasaka, T. Organometal Halide Perovskites as Visible-Light Sensitizers for Photovoltaic Cells. *J. Am. Chem. Soc.* **2009**, *131*, 6050–6051. [CrossRef] [PubMed]
3. Graetzel, M.; Malinkiewicz, O.; Yella, A.; Lee, Y.H.; Mı, G.; Nazeeruddin, M.K.; Bolink, H.J. Perovskite Solar Cells Employing Organic Charge-Transport Layers. *Nat. Photonics* **2014**, *8*, 128–132. [CrossRef]
4. Zh, O.; Yerezhep, D.; Aldiyarov, A.; Golikov, O.; Tokmoldin, N. Performance Simulation of Eco-Friendly Solar Cells Based on $CH_3NH_3SnI_3$. *Eurasian Phys. Tech. J.* **2022**, *19*, 58–64. [CrossRef]
5. Deepthi Jayan, K.; Sebastian, V. Comprehensive Device Modelling and Performance Analysis of $MASnI_3$ Based Perovskite Solar Cells with Diverse ETM, HTM and Back Metal Contacts. *Sol. Energy* **2021**, *217*, 40–48. [CrossRef]
6. Rawat, S.; Shrivastav, N.; Madan, J. Analysis and Optimization of $MASnPbI_3$-Based Single Junction Solar Cells for High Power Conversion Efficiency. In Proceedings of the 2023 Second International Conference on Electrical, Electronics, Information and Communication Technologies (ICEEICT), Trichirappalli, India, 5–7 April 2023; pp. 1–3. [CrossRef]
7. Shankar, G.; Kumar, P.; Pradhan, B. All-Perovskite Two-Terminal Tandem Solar Cell with 32.3% Efficiency by Numerical Simulation. *Mater. Today Sustain.* **2022**, *20*, 100241. [CrossRef]
8. Burgelman, M.; Nollet, P.; Degrave, S. Modelling Polycrystalline Semiconductor Solar Cells. *Thin Solid Films* **2000**, *361*, 527–532. [CrossRef]
9. Anwar, F.; Mahbub, R.; Satter, S.S.; Ullah, S.M. Effect of Different HTM Layers and Electrical Parameters on ZnO Nanorod-Based Lead-Free Perovskite Solar Cell for High-Efficiency Performance. *Int. J. Photoenergy* **2017**, *2017*, 9846310. [CrossRef]
10. Takahashi, Y.; Obara, R.; Lin, Z.; Takahashi, Y. Charge-Transport in Tin-Iodide Perovskite $CH_3NH_3SnI_3$: Origin of High Conductivity Takahashi. *Dalt. Trans.* **2011**, *40*, 5563–5568. [CrossRef] [PubMed]
11. Sabetvand, R.; Ghazi, M.E.; Izadifard, M. Studying Temperature Effects on Electronic and Optical Properties of Cubic $CH_3NH_3SnI_3$ Perovskite. *J. Comput. Electron.* **2020**, *19*, 70–79. [CrossRef]
12. Slami, A. Comparative Study of Modeling of Perovskite Solar Cell with Different HTM Layers. *Int. J. Mater.* **2020**, *7*, 2313–10555. [CrossRef]
13. Rühle, S. Tabulated Values of the Shockley-Queisser Limit for Single Junction Solar Cells. *Sol. Energy* **2016**, *130*, 139–147. [CrossRef]
14. Omarova, Z.; Yerezhep, D.; Aldiyarov, A.; Tokmoldin, N. In Silico Investigation of the Impact of Hole-Transport Layers on the Performance of $CH_3NH_3SnI_3$ Perovskite Photovoltaic Cells. *Crystals* **2022**, *12*, 699. [CrossRef]
15. Du, H.J.; Wang, W.C.; Zhu, J.Z. Device Simulation of Lead-Free CH3NH3SnI3 Perovskite Solar Cells with High Efficiency. *Chinese Phys. B* **2016**, *25*, 108802. [CrossRef]
16. Reyes, A.C.P.; Lázaro, R.C.A.; Leyva, K.M.; López, J.A.L.; Méndez, J.F.; Jiménez, A.H.H.; Zurita, A.L.M.; Carrillo, F.S.; Durán, E.O. Study of a Lead-Free Perovskite Solar Cell Using CZTS as HTL to Achieve a 20% PCE by SCAPS-1D Simulation. *Micromachines* **2021**, *12*, 1508. [CrossRef]
17. Dang, Y.; Zhou, Y.; Liu, X.; Ju, D.; Xia, S.; Xia, H.; Tao, X. Formation of Hybrid Perovskite Tin Iodide Single Crystals by Top-Seeded Solution Growth. *Angew. Chem. Int. Ed.* **2016**, *55*, 3447–3450. [CrossRef] [PubMed]

18. Ahamed, T.; Rahaman, I.; Karmakar, S.; Halim, A.; Kumar, P. Thickness Optimization and the Effect of Different Hole Transport Materials on Methylammonium Tin Iodide ($CH_3NH_3SnI_3$)-Based Perovskite Solar Cell. *Emergent Mater.* **2022**, *6*, 175–183. [CrossRef]
19. Zandi, S.; Razaghi, M. Finite Element Simulation of Perovskite Solar Cell: A Study on Efficiency Improvement Based on Structural and Material Modification. *Sol. Energy* **2019**, *179*, 298–306. [CrossRef]
20. Bouri, N.; Talbi, A.; Khaaissa, Y.; Derbali, S.; Bouich, A.; Nouneh, K. Insight into $MAPb_{1-x}Eu_xI_3$ Based Perovskite Solar Cell Performance Using SCAPS Simulator. *Optik* **2022**, *271*, 170235. [CrossRef]
21. Hasnain, S.M. Examining the Advances, Obstacles, and Achievements of Tin-Based Perovskite Solar Cells: A Review. *Sol. Energy* **2023**, *262*, 111825. [CrossRef]